INORGANIC CHEMISTRY FRONTIERS

RESEARCH ARTICLE

View Article Online
View Journal | View Issue

Cite this: *Inorg. Chem. Front.*, 2024, **11**, 3494

An unprecedented Cu_6 cluster-based bimetallic MOF with multiple open sites for high CO_2 capture and efficient CO_2 conversion†

Xueyue Yu,[a] Jiaming Gu,[a] Baobing Tang,[a] Tong Xu,[a] Guanghua Li,[a] Zhiyong Chang*[b,c] and Yunling Liu *[a]

Received 18th March 2024,
Accepted 8th May 2024

DOI: 10.1039/d4qi00692e

rsc.li/frontiers-inorganic

Based on the soft–hard acid–base theory, a novel bimetallic MOF (**JLU-MOF108**) has been successfully synthesized through a one-pot synthesis method. **JLU-MOF108** is a mixed metal-based MOF, constructed from an unprecedented hexanuclear copper cluster (12-connected), indium metal center (4-connected) and a tetrazole-containing carboxylic acid ligand (3-connected), that exhibits a (3, 4, 12)-connected **xag** topology. In order to effectively enhance the CO_2 capture and cycloaddition catalytic performance, abundant open metal sites (OMSs), Lewis basic sites (LBSs) and specific pore sizes have been implanted in the **JLU-MOF108** structure. Fascinatingly, the expected mixed metal-based MOF material has a high OMS density and suitable pore volume. The results show that **JLU-MOF108** exhibits high CO_2 adsorption performance and excellent epichlorohydrin (ECH) catalysing capability in cycloaddition reactions. More importantly, the yield of ECH can reach up to 97%, which surpasses many reported MOF materials. Therefore, **JLU-MOF108** can be a good candidate material for cycloaddition reactions and CO_2 storage.

Introduction

Along with the increasing progress of society and industrial development, humans demand more and more energy consumption. Due to industrial manufacturing, a high level of carbon dioxide (CO_2) appears in the air, becoming a main cause of global warming. So far, the efficient capture and utilization of CO_2 has become a major concern for the world.[1–5] The presence of high CO_2 concentrations in industrial production can affect the complete combustion and conversion efficiency of fuels, leading to huge energy waste.[6–9] Over the past few years, the method of CO_2 cycloaddition reaction has garnered significant interest for its gentle and efficient approach for capturing CO_2, and the conversion from CO_2 and epoxides to cyclic carbonate through a cycloaddition reaction is an effective way of CO_2 utilization.[4,10–13] In order to successfully achieve carbon peak and neutrality targets and transform CO_2 into more valuable feedstocks, researchers have investigated various materials to capture, convert and utilize CO_2.[14–18]

Metal–organic frameworks (MOFs) are usually composed of inorganic secondary building units (SBUs) of metal ions or metal clusters with multidentate organic ligands through coordination bonds in a specific coordination mode, also known as porous coordination polymers, and usually possess large surface areas, tunable pore sizes, adjustable chemical functionalities, and well-defined metal nodes.[19–21] The above advantages endow them with diverse potential applications especially in catalysis. With the continuous development of industry, the targeted synthesis of MOFs applied in specific fields is particularly important. For catalysis, it is necessary to design and synthesize MOF-based catalysts with a large specific surface area and suitable pore size to provide an appropriate reaction environment, and it is also necessary to introduce corresponding active sites to ensure efficient non-homogeneous catalytic reactions.[22–27] Several key properties of MOFs can enhance their CO_2 capture capability: (1) ultra-high specific surface area and controllable pore size.[28,29] (2) By the design and synthesis of nitrogen atoms with specific functional sites, such as the introduction of Lewis basic sites (LBSs), *etc.*[30,31] (3) Open metal sites (OMSs) can be seen as

[a]*State Key Laboratory of Inorganic Synthesis and Preparative Chemistry, College of Chemistry, Jilin University, Changchun 130012, P. R. China. E-mail: yunling@jlu.edu.cn*
[b]*Key Laboratory of Bionic Engineering, Ministry of Education, Jilin University, Changchun 130022, P. R. China. E-mail: zychang@jlu.edu.cn*
[c]*College of Biological and Agricultural Engineering, Jilin University, Changchun 130022, P. R. China. E-mail: zychang@jlu.edu.cn*

†Electronic supplementary information (ESI) available: PXRD patterns, gas adsorption measurement data, TGA analyses, ^{1}H NMR data, and catalytic reaction details. CCDC 2338522. For ESI and crystallographic data in CIF or other electronic format see DOI: **https://doi.org/10.1039/d4qi00692e**

Lewis acid sites (LASs) and they can polarize gas molecules such as carbon dioxide, thus enhancing the interaction of gases such as carbon dioxide with MOFs.[32–34] However, many catalysts have been reported, including some MOF-based materials, which usually need high work pressures (up to 3 MPa or higher) and high temperatures. Thus, designing and synthesizing MOFs capable of efficiently capturing and converting CO_2 under mild conditions remains a challenge.

Mixed metal cluster MOFs, which are composed of one or more organic ligands and a variety of inorganic SBUs, can provide new ideas for the design and synthesis of functional MOFs. Most of the reported mixed metal cluster-based MOFs are synthesized by post-synthesis methods.[35–39] However, these methods are complicated and limit the diversity and topological structures of MOFs to a certain extent. In contrast, the one-pot synthesis method of MOFs based on the soft–hard acid–base theory not only enriches the variety of structural elements, connection modes and framework structures, but also brings broader application prospects for mixed metal cluster-based MOFs with their novel pore size.[40–44] Combining the superiorities of mixed metal cluster MOFs, the one-pot synthesis method and outstanding performances in catalysis, bimetallic MOFs are expected to be a new type of efficient catalyst.[45–47] On the one hand, bimetallic MOFs possess more diverse active sites than monometallic MOFs, which makes them exhibit excellent performance in catalysis.[41,45,47–49] On the other hand, organic ligands can covalently bond with two metal sites in a single node, which is conducive to improving their thermal and chemical stability.[50,51]

Considering all the problems above, a novel Cu–In-MOF material (**JLU-MOF108**) constructed from a hetero-tetrazole-containing carboxylic acid ligand H_3TZPA (H_3TZPA = 5-(4-(tetrazol-5-yl)phenyl)isophthalic acid) and mixed copper and indium metals was successfully synthesized by a one-pot solvothermal method.

Remarkably, the structure of **JLU-MOF108** possesses an unprecedented hexanuclear copper cluster $[Cu_6(\mu_6\text{-}Cl)(N\text{–}N)_{12}]$ SBU, which has not been found so far in copper-based SBUs (Scheme 1).[52,53] The versatile coordination modes and stable oxidation states of metallic copper facilitate the formation of multi-nuclear copper cluster motifs. The common copper clusters include the typical paddlewheel $[Cu_2(CO_2)_4]$,[54] the triangular trinuclear copper cluster $[Cu_3(\mu_3\text{-}OH)N_6]$,[55] the square planar tetranuclear copper halide cluster $[Cu_4Cl]^{7+}$,[56] and the bicrown hexanuclear copper cluster $[Cu_6N_{12}Cl_6]$ and so on.[57–59] In contrast, the hexanuclear copper cluster in **JLU-MOF108**, with twelve connections, is distinct from the commonly observed 12-connected hexanuclear Zr clusters or rare earth (RE) clusters.[60–64] While hexanuclear Zr/RE clusters are linked by carboxylate oxygen, the hexanuclear copper clusters in **JLU-MOF108** are linked by N–N bonds in the tetrazole ligands, representing exceedingly rare formation, which is similar to the recently reported triazole-ligand linked $Cd_6(\mu_6\text{-}Cl)(N\text{–}N)_{12}Cl_6$ cluster.[65]

The hexanuclear copper clusters in **JLU-MOF108** can be viewed as 12-connected nodes and linked with 3-connected ligands and 4-connected indium SBUs to form a (3, 4, 12)-connected **xag** topology. Notably, **JLU-MOF108** has a large number of OMSs (considered as LASs) and LBSs (N atoms on the ligand and exposed in the pore channel). Benefiting from these active sites, **JLU-MOF108** achieves a 97% conversion rate of epichlorohydrin (ECH) at 1 atm under rather mild conditions, which exceeds many reported MOF materials. Moreover, **JLU-MOF108** exhibited high CO_2 uptake at 273 and 298 K.

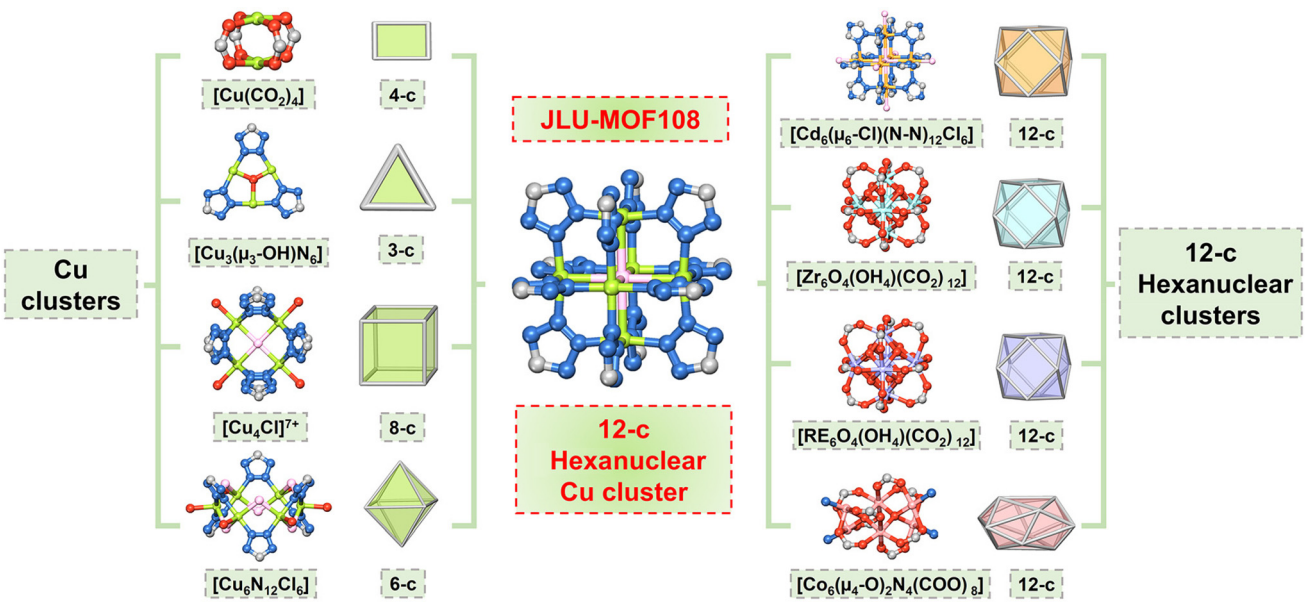

Scheme 1 Examples of Cu cluster-based MOFs with different connections and different hexanuclear metal cluster-based MOFs with 12 connections.

Experimental

Materials and methods

The organic ligands and other chemicals were commercially obtained without further purification. The analyses of C, H and N elements were carried out using a Vario MICRO Cube analyzer. Thermogravimetric analysis (TGA) was performed using a TGA Q500 machine at a heating rate of 10 °C min^{-1} under atmospheric pressure from room temperature to 800 °C. Powder X-ray diffraction (PXRD) data were collected through a Rigaku D/MAX2550 diffractometer, and Cu Kα radiation (λ = 1.5418 Å) was in the 2θ range of 3–40°. X-ray photoelectron spectroscopy (XPS) measurements were executed on an ESCALAB 250 X-ray photoelectron spectrometer and Mg Kα X-rays were used as the excitation source. IR spectra were recorded in the range of 400–4000 cm^{-1} on a Nicolet Impact 410 FTIR spectrometer using KBr pellets. The inductively coupled plasma (ICP) data were collected with a PerkinElmer Optima 3300 DV spectrometer.

X-ray crystallography

Single-crystal X-ray diffraction measurements for **JLU-MOF108** were obtained with a Bruker Apex II CCD diffractometer using graphite monochromatic Mo-Kα (λ = 0.71073 Å) radiation under atmospheric pressure and at room temperature. The structure of **JLU-MOF108** was solved by direct methods and refined by full-matrix least squares on F^2 in SHELXL-2014.[66] All non-hydrogen atoms were determined anisotropically. The formula was rooted in the crystallographic data associated with CHN elemental analyses and TGA data. The detailed crystallographic data and selected bond lengths and angles for the **JLU-MOF108** are listed in Tables S1 and S2.† Topology information for **JLU-MOF108** was obtained using TOPOS 4.0 software.[67]

Synthesis

$CuCl_2{\cdot}2H_2O$ (2 mg, 0.010 mmol), $In(NO_3)_3{\cdot}4H_2O$ (6 mg, 0.015 mmol) and H_3TZPA (3 mg, 0.010 mmol) were well dispersed in *N*,*N*-dimethylformamide (DMF) (1.0 mL) in a 20 mL vial. Then, deionized water (300 μL) was added to the solution and sonicated for 3 min. Finally, the mixture was heated at 115 °C for 24 h. Brown polyhedral single crystals were obtained and washed with DMF several times (74% yield based on the H_3TZPA ligand). Elemental analyses calculated (%): C, 44.67; H, 4.96; N, 15.05. Found (%): C, 44.39; H, 4.69; N, 15.42.

Gas adsorption measurements

The as-synthesized **JLU-MOF108** samples were exchanged by methanol solution 12 times in 2 days and then activated at 70 °C for 10 hours. The N_2 adsorption/desorption isotherm at 77 K was carried out on a Micromeritics ASAP 2420 instrument. The adsorption/desorption isotherms of CO_2, CH_4, C_2H_6, and C_3H_8 at 273 and 298 K were performed on a Micromeritics 3Flex.

Reactions of CO_2-epoxide cycloaddition

In a general atmospheric pressure catalytic reaction, activated **JLU-MOF108**, all epoxides (20 mmol) and co-catalysts (TBAB, 5 mol%) were placed in a clean 15 mL Schlenk tube. The tube was emptied of air before carbon dioxide was injected. A total of three evacuations were required to ensure that the tube was fully filled with carbon dioxide. The mixture was stirred under relatively mild conditions at 25 °C for propylene oxide (PO) and 80 °C for ECH, styrene oxide (SO) and other epoxides. The amount of catalyst in each catalytic reaction was calculated based on the number of OMSs. The catalysts were recovered after centrifugal separation in preparation for the next catalytic cycle. The final yields were determined and calculated by ^{1}H-NMR (*n*-dodecane was selected as an internal standard for PO).

Results and discussion

Structural description

The X-ray single-crystal structure reveals that **JLU-MOF108** crystallizes in the cubic crystal system, specifically belonging to the $Im\bar{3}m$ space group. As shown in Fig. 1 and Fig. S1,† **JLU-MOF108** is a bimetallic MOF material constructed from mixed-metal copper clusters and indium units, which contains three types of SBUs: a rare hexanuclear copper cluster structural motif, a mononuclear indium structural motif, and an organic structural motif with N and O donors. The hexanuclear copper cluster is an octahedron composed of six copper atoms, one Cl atom located at the centre of the cluster, and twelve N–N fragments at the bottom of twelve tetrazole ligands. The edge of the octahedron is connected by twelve N–N fragments, making it a hexacore copper cluster structure with twelve connections. This hexanuclear copper cluster SBU has not been found so far, and it is similar to the Cd_6 clusters in the reported PMo_{12}@CdMOF.[65] The nitrogen-containing portion of the H_3TZPA ligand is coordinated to copper, and the carboxylic oxygen at the other end is coordinated to the indium centre. Each In^{3+} chelated to four carboxylic oxygen atoms from different ligands, forming a 4-connected [$In(COO)_4$] structural motif. The organic ligand H_3TZPA containing a tetrazole group with a resorcylic acid moiety can be viewed as a 3-connected triangle node. From a topological viewpoint, **JLU-MOF108** shows a (3, 4, 12)-connected **xag** topology with the point symbol $\{6^{24}{\cdot}8^{12}{\cdot}10^{24}{\cdot}12^{6}\}\{6^{3}\}_{12}\{6^{4}{\cdot}8^{2}\}$. Although indium has no OMSs to assist in catalysis, the structure cannot form a three-dimensional structure when the mononuclear indium structural motif is removed, and thus the indium center acts as a connecting bridge.

In the [010] direction, there is a triangular window with a size of about 10.0 Å × 5.1 Å. **JLU-MOF108** has a cage-like structure in which each Cu_6 cluster is surrounded by six equal-sized cage-like structures. Each cage is composed of two Cu_6 clusters, four mononuclear indium units and eight ligands with a window size of about 20.0 Å × 10.0 Å. The space-filling view of

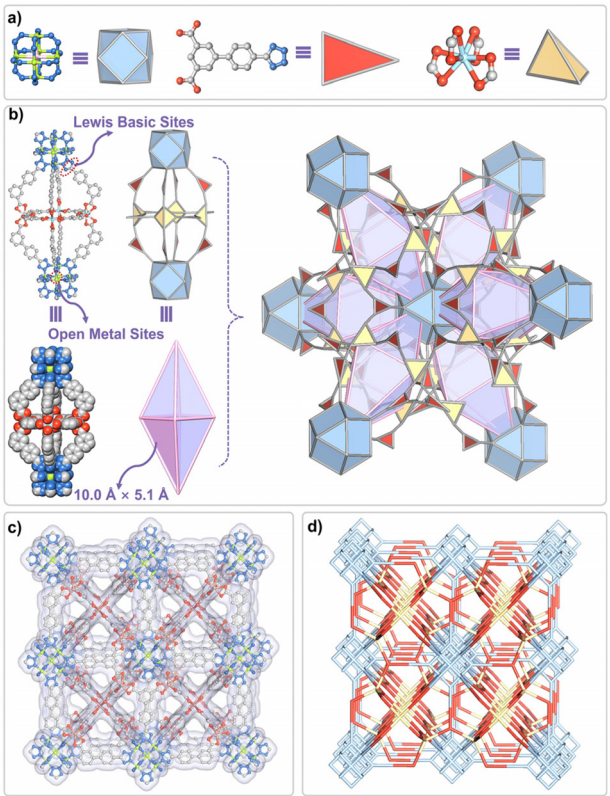

Fig. 1 Crystal structure of **JLU-MOF108**. (a) Simplification of the hexanuclear copper cluster SBU, indium SBU and organic ligand, (b) polyhedral view of the cage, (c) ball–stick and Connolly view of the channel along the [010] direction, and (d) topological view. Color scheme: carbon = gray, nitrogen = blue, oxygen = red, copper = green, indium = light blue, and chlorine = pink.

JLU-MOF108 with multiple pores along the [001] and [111] directions is shown in Fig. S2.†

The above structural analysis and characterization indicated that **JLU-MOF108** exhibits a high CO_2 adsorption capacity due to its high pore volume, cage structural motif and OMSs. Besides, there are a large number of OMSs and uncoordinated LBSs on the ligands, both of which can synergistically improve the CO_2 cycloaddition reaction catalytic effect.

Gas adsorption and separation behaviour

In order to explore the permanent porosity and surface area of **JLU-MOF108**, the nitrogen adsorption test on the sample was carried out at 77 K. Since **JLU-MOF108** is stable in acetonitrile, methanol, ethanol, acetone and dichloromethane solvents according to the PXRD pattern (Fig. S3†), the TGA analysis results (Fig. S4†) showed that methanol-exchanged **JLU-MOF108** could be completely activated at 70 °C. As shown in Fig. 2a, the nitrogen adsorption curve is a typical type I adsorption isotherm, which is consistent with the characteristics of microporous materials. The Brunauer–Emmett–Teller (BET) surface area is 1893 $m^2\ g^{-1}$, and the experimental pore volume is 0.90 $cm^3\ g^{-1}$, which is close to the theoretical value of 0.93 $cm^3\ g^{-1}$. The calculated pore size by using nonlocal

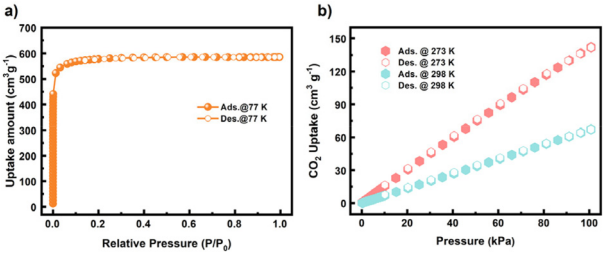

Fig. 2 (a) N_2 adsorption–desorption isotherm of **JLU-MOF108** at 77 K and (b) CO_2 adsorption–desorption isotherms of **JLU-MOF108** at 273 K and 298 K.

density functional theory (NLDFT) agrees well with the measured one of the **JLU-MOF108** structure (Fig. S5†). Due to the cage-like structure and OMSs in **JLU-MOF108**, it has a high carbon dioxide adsorption capacity. At 273 K and 298 K, the CO_2 absorption capacities are 141.9 $cm^3\ g^{-1}$ (6.3 mmol g^{-1}) and 67.2 $cm^3\ g^{-1}$ (3.0 mmol g^{-1}), as shown in Fig. 2b and Fig. S6,† and exceed many of the reported materials such as NH_2-MIL-125,[68] USTC-253,[69] MAF-23,[70] JNU-2,[71] and ZNU-1,[72] (Tables S3 and S4†). Then the gas adsorption test was conducted on the main component of natural gas CH_4 and the common impurities C_2H_6 and C_3H_8 (Fig. S7–S9†). At 1 atm, 273 and 298 K, the maximum adsorption capacities of CH_4 are 29.6 and 15.8 $cm^3\ g^{-1}$, respectively, while the maximum adsorption capacities of C_2H_6 are 190.3 and 134.7 $cm^3\ g^{-1}$, and the maximum adsorption capacities of C_3H_8 are 200.8 and 177.8 $cm^3\ g^{-1}$. Correspondingly, the experimental gas adsorption isotherms at 298 K were fitted with the DSLF equation, and the theoretical selectivities of binary gas mixtures were calculated by utilizing ideal adsorbed solution theory (IAST). According to Fig. S10,† in **JLU-MOF108** at 298 K and 1 atm, the adsorption selectivities of CO_2/CH_4 are 4.5 (0.5/0.5) and 4.8 (0.05/0.95). The adsorption selectivity of C_2H_6/CH_4 is 13.3 (0.5/0.5). The adsorption selectivity of C_3H_8/CH_4 reaches 248.2 (0.5/0.5) and exceeds many of the reported materials. Therefore, the results showed that **JLU-MOF108** exhibited good adsorption and separation capabilities.

CO_2 cycloaddition reactions

Based on the high CO_2 adsorption capacity of **JLU-MOF108**, further cycloaddition reactions were performed. First, the smallest propylene oxide (PO) was selected to explore its cycloaddition reaction performance (Table S6†). A series of exploratory experiments were carried out to find the optimal conditions for the catalytic reaction, as shown in Table 1. Firstly, 20 mmol PO was added, and the yield was only 15% after 12 hours at 1 bar and 25 °C without a catalyst. Then, when TBAB and **JLU-MOF108** were added alone, the yield also remained 25% and 20%, respectively. This indicates that the simultaneous presence of the co-catalyst and **JLU-MOF108** would be more favorable to the reaction. Therefore, the optimal conditions of **JLU-MOF108** for catalyzing the cycloaddition reaction of PO were obtained by varying the amounts

Table 1 JLU-MOF108 for the CO_2 cycloaddition reaction with PO under different conditions

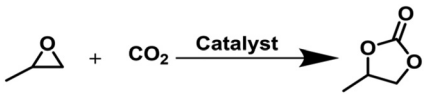

Entry	Catalyst	Tem./°C	P/bar	Time/h	Yield/%
1	None	25	1	12	15
2	Only TBAB	25	1	12	25
3	Only **JLU-MOF108**	25	1	12	20
4	**JLU-MOF108**[a]	25	1	12	68
5	**JLU-MOF108**[b]	25	1	12	73
6	**JLU-MOF108**[c]	25	1	12	99

[a] Reaction conditions: 20 mmol PO, 0.12 mol% open Cu sites of activated **JLU-MOF108**, and 2 mol% TBAB. [b] 0.25 mol% open Cu sites of activated **JLU-MOF108** and 2.5 mol% TBAB. [c] 0.25 mol% open Cu sites of activated **JLU-MOF108** and 5 mol% TBAB. Checked by ^{1}H NMR spectroscopy and *n*-dodecane was added as an internal standard.

of catalyst and co-catalyst: the addition of 5 mol% TBAB and 0.25 mol% OMSs of **JLU-MOF108** for 12 h at 1 bar and 25 °C catalyzes the conversion of 20 mmol PO with a yield of 99% (Fig. S13†). As shown in Table 2 and Fig. 3, the conversion of the ECH cycloaddition reaction can reach up to 97% by adding 5 mol% TBAB and **JLU-MOF108** (0.25 mol% OMSs) at 1 bar and 80 °C for 12 h (Fig. S14†). The TON (turnover number) and TOF (turnover frequency) values are 388 and 32.3 h^{-1}, which are higher than most of the reported MOF-based materials such as PCN-700-Me_2,[73] FJI-C10,[74] and JLU-Liu21[75] (Table S5†). However, the catalytic performances of the other four substrates were not very good, with yields ranging from 15 to 65% (Fig. S15–S18†). Therefore, the material has catalytic selectivity for small-sized substrates as illustrated in Table 3.

There are two types of functional sites in **JLU-MOF108**: the unsaturated metal Cu site (regarded as LASs) and the N atom (regarded as LBSs in the H_3TZPA ligand). Therefore, according to the relevant reports,[76–78] we proposed a possible catalytic mechanism of **JLU-MOF108** in the CO_2 cycloaddition reaction (Fig. 4). First, the nitrogen atoms in the epoxide can be trapped and polarized by the open Cu sites on the Cu_6 clus-

Table 2 JLU-MOF108 for the CO_2 cycloaddition reaction with ECH under different conditions

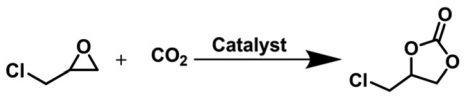

Entry	Catalyst	Tem./°C	P/bar	Time/h	Yield/%
1	**JLU-MOF108**[a]	80	1	12	53
2	**JLU-MOF108**[b]	80	1	12	73
3	**JLU-MOF108**[c]	80	1	12	97

[a] Reaction conditions: 20 mmol ECH, 0.12 mol% open Cu sites of activated **JLU-MOF108**, and 2 mol% TBAB. [b] 0.25 mol% open Cu sites of activated **JLU-MOF108** and 2.5 mol% TBAB. [c] 0.25 mol% open Cu sites of activated **JLU-MOF108** and 5 mol% TBAB. Checked by ^{1}H NMR spectroscopy and *n*-dodecane was added as an internal standard.

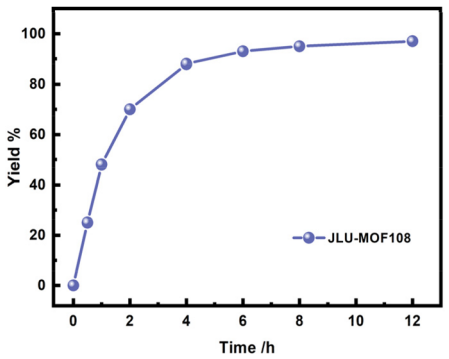

Fig. 3 Kinetic curve of CO_2–ECH cycloaddition catalyzed by **JLU-MOF108**.

Table 3 JLU-MOF108 for different epoxides for CO_2 cycloaddition reactions under optimal conditions

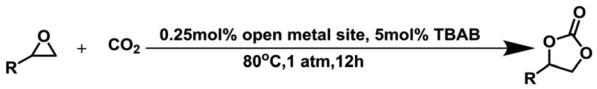

Entry	Epoxide	Product	Yield (%)
1			99
2			97
3			65
4			48
5			46
6			15

Catalytic performances were checked by ^{1}H NMR, and *n*-dodecane was added as the internal standard for PO.

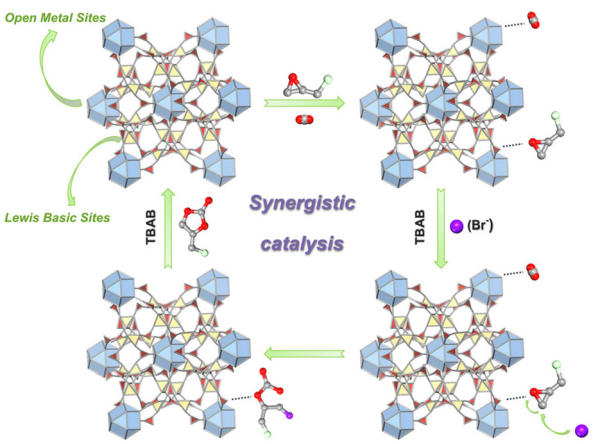

Fig. 4 A possible synergetic catalytic mechanism of **JLU-MOF108** in the CO_2–ECH catalytic cycloaddition reaction.

ters, thereby activating the epoxy ring. Then, the bromide ion in TBAB acts as a nucleophile to attack the epoxide, forming an epoxide anion intermediate and activating the adjacent CO_2 molecule to form a coordination bond with its contained carbon atom. Subsequently, the oxygen in the activated CO_2 attacks the carbon coordinated to the bromide ion to complete the cyclization and generate the product. Then, the nitrogen atom of tetrazole in the ligand H_3TZPA acts as a LBS to polarize CO_2 and form a coordination bond, and the electronegative oxygen in CO_2 attacks the epoxide to activate and open the ring. Finally, the oxygen in the epoxide attacks the carbon coordinated to the nitrogen, completing the cyclization. In conclusion, LASs and LBSs in **JLU-MOF108** synergistically catalyze the whole reaction process.

The recyclability performance is also an important index for evaluating the catalytic capability. Therefore, we investigated the recyclability of **JLU-MOF108** for the catalytic conversion of epichlorohydrin. The yield still remained at about 93% after four cycles. The PXRD pattern of the sample after four cycles further confirmed its stability, as shown in Fig. S11.† The IR and XPS spectra of **JLU-MOF108** after recycling 4 times are shown in Fig. S12.† ICP-OES analysis revealed that there were no Cu^{2+} and In^{3+} ions leaking from **JLU-MOF108** (Table S7†).

Overall, **JLU-MOF108** exhibits good catalytic selectivity due to the limiting effect of pore size, which further confirms that the material is a suitable catalyst for CO_2 immobilization.

Conclusions

In conclusion, a new bimetallic copper–indium metal–organic framework (**JLU-MOF108**) was designed and synthesized using a one-pot synthesis strategy. The framework exhibits a rare Cu_6 cluster structural motif due to the diversity of coordination modes, which exposes a large number of OMSs. Additionally, the nitrogen-containing carboxylic acid ligand provides uncoordinated LBSs. The unique cage-like structure of **JLU-MOF108** gives it excellent catalytic ability and high CO_2 capture capacity. The bimetallic mixed-MOF design demonstrates the potential for introducing numerous OMSs into the MOF structure to enhance catalytic ability. This provides guidance for future work in this field.

Conflicts of interest

There are no conflicts to declare.

Acknowledgements

This work was supported by the National Natural Science Foundation of China (No. 22171100 and U23A20360) and the '111 Center' (B17020).

References

1 A. Goeppert, M. Czaun, J. P. Jones, G. K. Surya Prakash and G. A. Olah, Recycling of carbon dioxide to methanol and derived products - closing the loop, *Chem. Soc. Rev.*, 2014, **43**, 7995–8048.
2 Z. Liu, D. B. Guan, W. Wei, S. Davis, P. Ciais, J. Bai, S. S. Peng, Q. Zhang, K. Hubacek, G. Marland, R. Andres, D. Crawford-Brown, J. T. Lin, H. Y. Zhao, C. P. Hong, T. Boden, K. S. Feng, G. Peters, F. M. Xi, J. G. Liu, Y. Li, Y. Zhao, N. Zeng and K. He, Reduced carbon emission estimates from fossil fuel combustion and cement production in China, *Nature*, 2015, **524**, 335–338.
3 M. Arslan, G. Tian, B. Ali, C. Zhang, H. Xiong, Z. Li, L. Luo, X. Chen and F. Wei, Highly selective conversion of CO_2 or CO into precursors for kerosene-based aviation fuel via an aldol–aromatic mechanism, *ACS Catal.*, 2022, **12**, 2023–2033.
4 G. Singh, J. Lee, A. Karakoti, R. Bahadur, J. Yi, D. Zhao, K. AlBahily and A. Vinu, Emerging trends in porous materials for CO_2 capture and conversion, *Chem. Soc. Rev.*, 2020, **49**, 4360–4404.
5 T. K. Pal, D. De and P. K. Bharadwaj, Metal–organic frameworks for the chemical fixation of CO_2 into cyclic carbonates, *Coord. Chem. Rev.*, 2020, **408**, 213173.
6 F. N. Al-Rowaili, U. Zahid, S. Onaizi, M. Khaled, A. Jamal and E. M. Al-Mutairi, A review for metal-organic frameworks (MOFs) utilization in capture and conversion of carbon dioxide into valuable products, *J. CO_2 Util.*, 2021, **53**, 101715.
7 S. N. Talapaneni, G. Singh, I. Y. Kim, K. AlBahily, A. H. Al-Muhtaseb, A. S. Karakoti, E. Tavakkoli and A. Vinu, Nanostructured carbon nitrides for CO_2 capture and conversion, *Adv. Mater.*, 2020, **32**, e1904635.
8 H. Ou, S. Ning, P. Zhu, S. Chen, A. Han, Q. Kang, Z. Hu, J. Ye, D. Wang and Y. Li, Carbon nitride photocatalysts with integrated oxidation and reduction atomic active centers for improved CO_2 conversion, *Angew. Chem., Int. Ed.*, 2022, **61**, e202206579.
9 W. D. Jones, Carbon capture and conversion, *J. Am. Chem. Soc.*, 2020, **142**, 4955–4957.
10 C. A. Trickett, A. Helal, B. A. Al-Maythalony, Z. H. Yamani, K. E. Cordova and O. M. Yaghi, The chemistry of metal–organic frameworks for CO_2 capture, regeneration and conversion, *Nat. Rev. Mater.*, 2017, **2**, 17045.
11 J. Liu, P. K. Thallapally, B. P. McGrail, D. R. Brown and J. Liu, Progress in adsorption-based CO_2 capture by metal-organic frameworks, *Chem. Soc. Rev.*, 2012, **41**, 2308–2322.
12 Z. Zhang, Z.-Z. Yao, S. Xiang and B. Chen, Perspective of microporous metal–organic frameworks for CO_2 capture and separation, *Energy Environ. Sci.*, 2014, **7**, 2868–2899.
13 J. Yu, L. H. Xie, J. R. Li, Y. Ma, J. M. Seminario and P. B. Balbuena, CO_2 capture and separations using MOFs: computational and experimental studies, *Chem. Rev.*, 2017, **117**, 9674–9754.

14 R. Luo, Y. Yang, K. Chen, X. Liu, M. Chen, W. Xu, B. Liu, H. Ji and Y. Fang, Tailored covalent organic frameworks for simultaneously capturing and converting CO_2 into cyclic carbonates, *J. Mater. Chem. A*, 2021, **9**, 20941–20956.
15 J. B. Lin, T. T. T. Nguyen, R. Vaidhyanathan, J. Burner, J. M. Taylor, H. Durekova, F. Akhtar, R. K. Mah, O. Ghaffari-Nik, S. Marx, N. Fylstra, S. S. Iremonger, K. W. Dawson, P. Sarkar, P. Hovington, A. Rajendran, T. K. Woo and G. K. H. Shimizu, A scalable metal-organic framework as a durable physisorbent for carbon dioxide capture, *Science*, 2021, **374**, 1464–1469.
16 D. Feng, W. C. Chung, Z. Wei, Z. Y. Gu, H. L. Jiang, Y. P. Chen, D. J. Darensbourg and H. C. Zhou, Construction of ultrastable porphyrin Zr metal-organic frameworks through linker elimination, *J. Am. Chem. Soc.*, 2013, **135**, 17105–17110.
17 G. Cai, M. Ding, Q. Wu and H.-L. Jiang, Encapsulating soluble active species into hollow crystalline porous capsules beyond integration of homogeneous and heterogeneous catalysis, *Natl. Sci. Rev.*, 2020, **7**, 37–45.
18 S. Gulati, S. Vijayan, Mansi, S. Kumar, B. Harikumar, M. Trivedi and R. S. Varma, Recent advances in the application of metal-organic frameworks (MOFs)-based nanocatalysts for direct conversion of carbon dioxide (CO_2) to value-added chemicals, *Coord. Chem. Rev.*, 2023, **474**, 214853.
19 H. C. Zhou and S. Kitagawa, Metal-organic frameworks (MOFs), *Chem. Soc. Rev.*, 2014, **43**, 5415–5418.
20 M. O'Keeffe and O. M. Yaghi, Deconstructing the crystal structures of metal-organic frameworks and related materials into their underlying nets, *Chem. Rev.*, 2012, **112**, 675–702.
21 H. Furukawa, K. E. Cordova, M. O'Keeffe and O. M. Yaghi, The chemistry and applications of metal-organic frameworks, *Science*, 2013, **341**, 1230444.
22 J. Lee, O. K. Farha, J. Roberts, K. A. Scheidt, S. T. Nguyen and J. T. Hupp, Metal-organic framework materials as catalysts, *Chem. Soc. Rev.*, 2009, **38**, 1450–1459.
23 S. Yuan, L. Feng, K. Wang, J. Pang, M. Bosch, C. Lollar, Y. Sun, J. Qin, X. Yang, P. Zhang, Q. Wang, L. Zou, Y. Zhang, L. Zhang, Y. Fang, J. Li and H. C. Zhou, Stable metal-organic frameworks: design, synthesis, and applications, *Adv. Mater.*, 2018, **30**, e1704303.
24 M. Ding, R. W. Flaig, H. L. Jiang and O. M. Yaghi, Carbon capture and conversion using metal-organic frameworks and MOF-based materials, *Chem. Soc. Rev.*, 2019, **48**, 2783–2828.
25 L. Zhu, X. Q. Liu, H. L. Jiang and L. B. Sun, Metal-organic frameworks for heterogeneous basic catalysis, *Chem. Rev.*, 2017, **117**, 8129–8176.
26 J. R. Long and O. M. Yaghi, The pervasive chemistry of metal-organic frameworks, *Chem. Soc. Rev.*, 2009, **38**, 1213–1214.
27 H. C. Zhou, J. R. Long and O. M. Yaghi, Introduction to metal-organic frameworks, *Chem. Rev.*, 2012, **112**, 673–674.
28 H. Furukawa, N. Ko, Y. B. Go, N. Aratani, S. B. Choi, E. Choi, A. O. Yazaydin, R. Q. Snurr, M. O'Keeffe, J. Kim and O. M. Yaghi, Ultrahigh porosity in metal-organic frameworks, *Science*, 2010, **329**, 424–428.
29 H. Deng, S. Grunder, K. E. Cordova, C. Valente, H. Furukawa, M. Hmadeh, F. Gandara, A. C. Whalley, Z. Liu, S. Asahina, H. Kazumori, M. O'Keeffe, O. Terasaki, J. F. Stoddart and O. M. Yaghi, Large-pore apertures in a series of metal-organic frameworks, *Science*, 2012, **336**, 1018–1023.
30 Z. Yin, S. Wan, J. Yang, M. Kurmoo and M.-H. Zeng, Recent advances in post-synthetic modification of metal–organic frameworks: new types and tandem reactions, *Coord. Chem. Rev.*, 2019, **378**, 500–512.
31 J. T. Li, P. M. Bhatt, J. Y. Li, M. Eddaoudi and Y. Y. Liu, Recent progress on microfine design of metal-organic frameworks: structure regulation and gas sorption and separation, *Adv. Mater.*, 2020, **32**, 2002563.
32 J. Zhu, P. M. Usov, W. Xu, P. J. Celis-Salazar, S. Lin, M. C. Kessinger, C. Landaverde-Alvarado, M. Cai, A. M. May, C. Slebodnick, D. Zhu, S. D. Senanayake and A. J. Morris, A new class of metal-cyclam-based zirconium metal-organic frameworks for CO_2 adsorption and chemical fixation, *J. Am. Chem. Soc.*, 2018, **140**, 993–1003.
33 A. K. Gupta, N. Guha, S. Krishnan, P. Mathur and D. K. Rai, A three-dimensional Cu(II)-MOF with Lewis acid–base dual functional sites for chemical fixation of CO_2 via cyclic carbonate synthesis, *J. CO_2 Util.*, 2020, **39**, 101173.
34 W. Xiang, J. Ren, S. Chen, C. Shen, Y. Chen, M. Zhang and C.-j. Liu, The metal–organic framework UiO-66 with missing-linker defects: a highly active catalyst for carbon dioxide cycloaddition, *Appl. Energy*, 2020, **277**, 115560.
35 A. Bajpai, P. Chandrasekhar, S. Govardhan, R. Banerjee and J. N. Moorthy, Single crystal-to-single crystal site-selective postsynthetic metal exchange in a Zn-MOF based on semi-rigid tricarboxylic acid and access to bimetallic MOFs, *Chem. – Eur. J.*, 2015, **21**, 2759–2765.
36 A. A. Kassie, P. Duan, E. T. McClure, K. Schmidt-Rohr, P. M. Woodward and C. R. Wade, Postsynthetic metal exchange in a metal-organic framework assembled from Co(III) diphosphine pincer complexes, *Inorg. Chem.*, 2019, **58**, 3227–3236.
37 Y. Lee, S. Kim, J. K. Kang and S. M. Cohen, Photocatalytic CO_2 reduction by a mixed metal (Zr/Ti), mixed ligand metal-organic framework under visible light irradiation, *Chem. Commun.*, 2015, **51**, 5735–5738.
38 L. Jiang, J. Zhao, S. Chen, J. Li, D. Wu and Y. Li, A highly symmetric bimetallic-tetracarboxylate framework: two-step crystallization and gas separation properties, *Inorg. Chem.*, 2019, **58**, 9425–9431.
39 S. Abednatanzi, P. Gohari Derakhshandeh, H. Depauw, F. X. Coudert, H. Vrielinck, P. Van Der Voort and K. Leus, Mixed-metal metal-organic frameworks, *Chem. Soc. Rev.*, 2019, **48**, 2535–2565.
40 S. Yuan, J. S. Qin, J. Li, L. Huang, L. Feng, Y. Fang, C. Lollar, J. Pang, L. Zhang, D. Sun, A. Alsalme, T. Cagin

and H. C. Zhou, Retrosynthesis of multi-component metal-organic frameworks, *Nat. Commun.*, 2018, **9**, 808.

41 L. Chen, H. F. Wang, C. Li and Q. Xu, Bimetallic metal-organic frameworks and their derivatives, *Chem. Sci.*, 2020, **11**, 5369–5403.

42 B. Iqbal, M. Saleem, S. N. Arshad, J. Rashid, N. Hussain and M. Zaheer, One-pot synthesis of heterobimetallic metal-organic frameworks (MOFs) for multifunctional catalysis, *Chem. – Eur. J.*, 2019, **25**, 10490–10498.

43 W. Li, X. Guo, P. Geng, M. Du, Q. Jing, X. Chen, G. Zhang, H. Li, Q. Xu, P. Braunstein and H. Pang, Rational design and general synthesis of multimetallic metal-organic framework nano-octahedra for enhanced Li-S battery, *Adv. Mater.*, 2021, **33**, e2105163.

44 Q. G. Zhai, C. Mao, X. Zhao, Q. Lin, F. Bu, X. Chen, X. Bu and P. Feng, Cooperative crystallization of heterometallic indium–chromium metal–organic polyhedra and their fast proton conductivity, *Angew. Chem.*, 2015, **127**, 7997–8001.

45 Y. B. Huang, J. Liang, X. S. Wang and R. Cao, Multifunctional metal-organic framework catalysts: synergistic catalysis and tandem reactions, *Chem. Soc. Rev.*, 2017, **46**, 126–157.

46 S. Liu, Y. Qiu, Y. Liu, W. Zhang, Z. Dai, D. Srivastava, A. Kumar, Y. Pan and J. Liu, Recent advances in bimetallic metal–organic frameworks (BMOFs): synthesis, applications and challenges, *New J. Chem.*, 2022, **46**, 13818–13837.

47 I. Soni, P. Kumar and G. Kudur Jayaprakash, Recent advancements in the synthesis and electrocatalytic activity of two-dimensional metal–organic framework with bimetallic nodes for energy-related applications, *Coord. Chem. Rev.*, 2022, **472**, 214782.

48 Y.-Z. Chen, Y.-X. Zhou, H. Wang, J. Lu, T. Uchida, Q. Xu, S.-H. Yu and H.-L. Jiang, Multifunctional PdAg@Mil-101 for one-pot cascade reactions: combination of host–guest cooperation and bimetallic synergy in catalysis, *ACS Catal.*, 2015, **5**, 2062–2069.

49 K. R. Oh, H. Lee, G. N. Yun, C. Yoo, J. W. Yoon, A. Awad, H. W. Jeong and Y. K. Hwang, Fabrication of hierarchical, porous, bimetallic, zeolitic imidazolate frameworks with the incorporation of square planar Pd and its catalytic application, *ACS Appl. Mater. Interfaces*, 2023, **15**, 9296–9306.

50 L. Chen, H.-F. Wang, C. Li and Q. Xu, Bimetallic metal–organic frameworks and their derivatives, *Chem. Sci.*, 2020, **11**, 5369–5403.

51 S. Dang, Q.-L. Zhu and Q. Xu, Nanomaterials derived from metal–organic frameworks, *Nat. Rev. Mater.*, 2017, **3**, 17075.

52 D. J. Tranchemontagne, J. L. Mendoza-Cortés, M. O'Keeffe and O. M. Yaghi, Secondary building units, nets and bonding in the chemistry of metal–organic frameworks, *Chem. Soc. Rev.*, 2009, **38**, 1257.

53 O. M. Yaghi, M. O'Keeffe, N. W. Ockwig, H. K. Chae, M. Eddaoudi and J. Kim, Reticular synthesis and the design of new materials, *Nature*, 2003, **423**, 705–714.

54 F. Nouar, J. F. Eubank, T. Bousquet, L. Wojtas, M. J. Zaworotko and M. Eddaoudi, Supermolecular building blocks (SBBs) for the design and synthesis of highly porous metal-organic frameworks, *J. Am. Chem. Soc.*, 2008, **130**, 1833–1835.

55 J. F. Eubank, F. Nouar, R. Luebke, A. J. Cairns, L. Wojtas, M. Alkordi, T. Bousquet, M. R. Hight, J. Eckert, J. P. Embs, P. A. Georgiev and M. Eddaoudi, On demand: the singular rht net, an ideal blueprint for the construction of a metal-organic framework (MOF) platform, *Angew. Chem., Int. Ed.*, 2012, **51**, 10099–10103.

56 D. Wang, T. Zhao, G. Li, Q. Huo and Y. Liu, A porous sodalite-type MOF based on tetrazolcarboxylate ligands and $[Cu_4Cl]^{7+}$ squares with open metal sites for gas sorption, *Dalton Trans.*, 2014, **43**, 2365–2368.

57 J. Yuan, J. Li, S. Che, G. Li, X. Liu, X. Sun, L. Zou, L. Zhang and Y. Liu, Two unique copper cluster-based metal–organic frameworks with high performance for CO_2 adsorption and separation, *Inorg. Chem. Front.*, 2019, **6**, 556–561.

58 D. Wang, J. Zhang, G. Li, J. Yuan, J. Li, Q. Huo and Y. Liu, Mesoporous hexanuclear copper cluster-based metal-organic framework with highly selective adsorption of gas and organic dye molecules, *ACS Appl. Mater. Interfaces*, 2018, **10**, 31233–31239.

59 S. Yao, T. Xu, N. Zhao, L. Zhang, Q. Huo and Y. Liu, An anionic metal-organic framework with ternary building units for rapid and selective adsorption of dyes, *Dalton Trans.*, 2017, **46**, 3332–3337.

60 D. Feng, Z. Y. Gu, Y. P. Chen, J. Park, Z. Wei, Y. Sun, M. Bosch, S. Yuan and H. C. Zhou, A highly stable porphyrinic zirconium metal-organic framework with shp-a topology, *J. Am. Chem. Soc.*, 2014, **136**, 17714–17717.

61 H. Furukawa, F. Gandara, Y. B. Zhang, J. Jiang, W. L. Queen, M. R. Hudson and O. M. Yaghi, Water adsorption in porous metal-organic frameworks and related materials, *J. Am. Chem. Soc.*, 2014, **136**, 4369–4381.

62 J. Qiao, X. Liu, L. Zhang, J. F. Eubank, X. Liu and Y. Liu, Unique fluorescence turn-on and turn-off-on responses to acids by a carbazole-based metal-organic framework and theoretical studies, *J. Am. Chem. Soc.*, 2022, **144**, 17054–17063.

63 D. X. Xue, A. J. Cairns, Y. Belmabkhout, L. Wojtas, Y. Liu, M. H. Alkordi and M. Eddaoudi, Tunable rare-earth fcu-MOFs: a platform for systematic enhancement of CO_2 adsorption energetics and uptake, *J. Am. Chem. Soc.*, 2013, **135**, 7660–7667.

64 L. Liu, Z. Yao, Y. Ye, Y. Yang, Q. Lin, Z. Zhang, M. O'Keeffe and S. Xiang, Integrating the pillared-layer strategy and pore-space partition method to construct multicomponent MOFs for C_2H_2/CO_2 separation, *J. Am. Chem. Soc.*, 2020, **142**, 9258–9266.

65 J. Du, Y.-Y. Ma, W.-J. Cui, S.-M. Zhang, Z.-G. Han, R.-H. Li, X.-Q. Han, W. Guan, Y.-H. Wang, Y.-Q. Li, Y. Liu, F.-Y. Yu, K.-Q. Wei, H.-Q. Tan, Z.-H. Kang and Y.-G. Li, Unraveling photocatalytic electron transfer mechanism in polyoxometalate-encapsulated metal-organic frameworks for high-

efficient CO2 reduction reaction, *Appl. Catal., B*, 2022, **318**, 121812.
66 G. M. Sheldrick, Crystal structure refinement with SHELXL, *Acta Crystallogr., Sect. C: Struct. Chem.*, 2015, **71**, 3–8.
67 V. A. Blatov, A. P. Shevchenko and D. M. Proserpio, Applied topological analysis of crystal structures with the program package ToposPro, *Cryst. Growth Des.*, 2014, **14**, 3576–3586.
68 S.-N. Kim, J. Kim, H.-Y. Kim, H.-Y. Cho and W.-S. Ahn, Adsorption/catalytic properties of MIL-125 and NH_2-MIL-125, *Catal. Today*, 2013, **204**, 85–93.
69 Z. R. Jiang, H. Wang, Y. Hu, J. Lu and H. L. Jiang, Polar group and defect engineering in a metal-organic framework: synergistic promotion of carbon dioxide sorption and conversion, *ChemSusChem*, 2015, **8**, 878–885.
70 P. Q. Liao, D. D. Zhou, A. X. Zhu, L. Jiang, R. B. Lin, J. P. Zhang and X. M. Chen, Strong and dynamic CO_2 sorption in a flexible porous framework possessing guest chelating claws, *J. Am. Chem. Soc.*, 2012, **134**, 17380–17383.
71 W. Fan, S. Yuan, W. Wang, L. Feng, X. Liu, X. Zhang, X. Wang, Z. Kang, F. Dai, D. Yuan, D. Sun and H. C. Zhou, Optimizing multivariate metal-organic frameworks for efficient C_2H_2/CO_2 separation, *J. Am. Chem. Soc.*, 2020, **142**, 8728–8737.
72 L. Wang, W. Sun, Y. Zhang, N. Xu, R. Krishna, J. Hu, Y. Jiang, Y. He and H. Xing, Interpenetration symmetry control within ultramicroporous robust boron cluster hybrid mofs for benchmark purification of acetylene from carbon dioxide, *Angew. Chem., Int. Ed.*, 2021, **60**, 22865–22870.
73 S. Yuan, L. Zou, H. Li, Y. P. Chen, J. Qin, Q. Zhang, W. Lu, M. B. Hall and H. C. Zhou, Flexible zirconium metal-organic frameworks as bioinspired switchable catalysts, *Angew. Chem., Int. Ed.*, 2016, **55**, 10776–10780.
74 J. Liang, Y. Q. Xie, X. S. Wang, Q. Wang, T. T. Liu, Y. B. Huang and R. Cao, An imidazolium-functionalized mesoporous cationic metal-organic framework for cooperative CO_2 fixation into cyclic carbonate, *Chem. Commun.*, 2018, **54**, 342–345.
75 J. M. Gu, X. D. Sun, X. Y. Liu, Y. Yuan, H. Y. Shan and Y. L. Liu, Highly efficient synergistic CO_2 conversion with epoxide using copper polyhedron-based MOFs with Lewis acid and base sites, *Inorg. Chem. Front.*, 2020, **7**, 4517–4526.
76 X. Q. Huang, X. Y. Gu, H. C. Zhang, G. D. Shen, S. W. Gong, B. C. Yang, Y. L. Wang and Y. F. Chen, Decavanadate-based clusters as bifunctional catalysts for efficient treatment of carbon dioxide and simulant sulfur mustard, *J CO_2 Util.*, 2021, **45**, 101419.
77 X. Q. Huang, Y. F. Chen, Z. G. Lin, X. Q. Ren, Y. N. Song, Z. Z. Xu, X. M. Dong, X. G. Li, C. W. Hu and B. Wang, Zn-BTC MOFs with active metal sites synthesized via a structure-directing approach for highly efficient carbon conversion, *Chem. Commun.*, 2014, **50**, 2624–2627.
78 X. Z. Si, Q. X. Yao, X. Z. Pan, X. Y. Zhang, C. L. Zhang, Z. Q. Li, W. Z. Duan, J. L. Hou and X. Q. Huang, Mesoporous MOF based on a hexagonal bipyramid Co_8-cluster: high catalytic efficiency on the cycloaddition reaction of CO_2 with bulky epoxides, *Inorg. Chem.*, 2023, **62**, 15006–15014.